Academic Journal of Science and Technology
ISSN: 2771-3032 | Vol. 19, No. 1, 2026

Deployment Impact Analysis of a Certain Type of Folding Wing Deployment Mechanism

Pengfei Zhang *, Yanbin Qin

Xi'an Shiyou University, Xi'an Shaanxi, 710018, China

*** Corresponding author:** Pengfei Zhang

Abstract: The instantaneous impact problem of the folding wing when it is fully deployed is theoretically analyzed by using the impact theory in theoretical mechanics. The dynamic process simulation analysis of the contact impact part of the fully deployed folding wing is carried out by Ansys software. The impact force function is adopted to describe the impact effect between the shock absorber pad and the projectile wing, and the determination method of the force function parameters is given. The analysis results show that the modeling method in this paper is suitable for theoretically and numerically simulating the impact characteristics of the folding wing during full deployment. For the designed working condition with a maximum spring force of 525 N, through analyzing the dynamic characteristics of the projectile wing and the buffer pad within the 8 mm impact stroke, the impact time is obtained as 0.1 s, the peak impact stress is 7.7 MPa, and the peak impact force is 770 N, which is less than the design upper limit of 5000 N and meets the safety requirements for the peak impact stress.

Keywords: Folding Wing; Collision; Buffering; Dynamic Simulation.

1. Introduction

Folding wings can reduce the size of aircraft, facilitate storage, transportation and launch, thereby improving the tactical and technical performance of weapon systems, and have been widely applied in modern aircraft. The deployment performance and buffering characteristics of in-position impact of folding wings are important technical indicators for folding wing design, which are related to the normal flight of aircraft. A certain type of folding wing adopts an elastic-driven mode as the power source for folding wing deployment. It utilizes compressed springs to generate elastic force, drives the movement of the guide sleeve piston, and then pulls the linkage mechanism to drive the folding wing to rotate and deploy around the fixed rotating shaft. Although the service life of springs is limited by the number of deployments, their structure is simple and reliable, consisting of a small number of components. This reduces the possibility of failures and improves the stability and reliability of the system. The lightweight design of springs helps reduce the overall weight of the aircraft and enhance flight performance. In addition, spring-driven deployment features fast response without the need for external energy input, which improves the independence and reliability of the system while reducing costs. Due to the short time required for deployment, the folding wing surface deployment process exhibits high dynamicity, resulting in the wing surface still having considerable kinetic energy after reaching the in-position state. Therefore, certain buffering measures must be taken to improve the locking reliability after reaching the designed angle and reduce the impact load upon in-positioning, and this load has an important influence on the flight stability and structural integrity of the aircraft.

Domestic and international research on the dynamic problems of folding wings mostly focuses on the dynamic analysis and experimental testing of their deployment process[1-8]. These studies mainly pay attention to the impact stress during the deployment process of folding wings or on the wing surface itself, and most of them do not involve the local dynamic problems of the in-position impact process of folding wings.

In this paper, the instantaneous impact problem of the folding wing at the moment of full deployment is theoretically analyzed by using the impact theory in theoretical mechanics. The dynamic process simulation analysis of the local contact-impact area of the fully deployed folding wing is carried out with Ansys software. The impact force function is applied to describe the impact interaction between the shock absorber pad and the guide sleeve, and the method for determining the parameters of the force function is proposed. On this basis, the in-position impact characteristics and influencing factors of a certain type of folding wing are studied.

2. Theoretical Analysis of In-position Impact of Folding Wings

A certain type of folding wing adopts a buffer pad as an auxiliary buffering device after the wing surface reaches the in-position state. The buffer pad is installed at the end of the guide shaft of the folding wing deployment mechanism and attached to the mounting plate. During the process of the projectile wing deploying to the in-position state, its impact surface collides with the buffer pad, and the buffering device takes effect first to mitigate the impact on the mounting plate. After the projectile wing is in position, the lock shaft in the locking mechanism is pushed by the spring force, and its tapered end is pressed into the tapered hole at the rotating shaft of the projectile wing to lock the wing in place. In this paper, the instantaneous impact problem is theoretically analyzed by using the impact theory in theoretical mechanics.

(1) Basic Assumptions

To simplify the research on the in-position impact problem of the projectile wing deployment, the following basic assumptions are proposed [10]:

1) Since the impact force is extremely large, far exceeding ordinary forces (e.g., gravity), the impulse of ordinary forces during the impact process can be neglected.

2) The impact duration is extremely short, and the positions

of the colliding objects are assumed to remain unchanged during the impact process.

3) Although the impact process takes a very short time, it still consists of two phases. The first phase, called the deformation phase, starts from the initial contact of the two objects, proceeds until the impact force reaches the maximum value, the two objects undergo maximum deformation, and there is no relative velocity between the two objects along the common normal direction at the contact point. The second phase, called the recovery phase, follows immediately: the objects partially or fully recover their original shapes due to elasticity until the two objects separate again. It is assumed here that each phase is completed instantaneously, i.e., the rigid-body impact assumption is adopted.

4) It is assumed that the deformation during the impact process is minimal, confined to a very small area near the contact point of the colliding objects, and completed instantaneously.

(2) Theoretical Analysis of In-position Impact

The impulse-momentum theorem during impact can be expressed by the formula:

$$\sum m_i u_i - \sum m_i v_i = \sum S_i \tag{1}$$

In the above formula: $\sum m_i u_i - \sum m_i v_i$ is the momentum change of the particle system during the impact process;

$\sum S_i$ is the vector sum of the external impact impulses acting on the particle system.

Neglecting the angular impulse of ordinary forces, the theorem of angular impulse and momentum of a particle system about a fixed axis during impact can be expressed by the formula:

$$\sum m_z(m_i u_i) - \sum m_z(m_i v_i) = \sum m_z(S_i) \tag{2}$$

In the above formula: $\sum m_z(m_i u_i) - \sum m_z(m_i v_i)$ is the change in the angular momentum of the particle system about the fixed axis Z during the impact process.

$\sum m_z(S_i)$ is the vector sum of the moments of the external impact impulses acting on the particle system about the same fixed axis Z.

Based on the impulse-momentum theorem and the theorem of angular impulse and momentum, the coefficient of restitution is introduced, and the kinetic energy loss during the central direct impact of two objects can be expressed by the formula[10]:

$$\Delta T = \frac{1}{2}\frac{m_1 m_2}{m_1 + m_2}(1 - e^2)(v_1 - v_2)^2 \tag{3}$$

In the above formula: ΔT is the kinetic energy loss during the central direct impact of the two objects;

e is the coefficient of restitution;

m1,m2,v1,v2 are the masses of object 1 and object 2 and their velocities immediately before the impact, respectively.

The folding wing is a rigid body rotating around a fixed axis subjected to impact, as shown in Figure 1. When a rigid body with a plane of symmetry rotates around the fixed axis OZ perpendicular to this plane of symmetry, if it is acted upon by an external impact impulse S within the plane of symmetry, then during the impact time interval τ, the angular velocity of the rigid body changes from ω to Ω. Meanwhile, an impact impulse SO is also generated at the bearing O, whose components along the x-axis and y-axis are SOx and SOy respectively. Assume that the moment of inertia of the rigid body about the z-axis is Iz , the x-axis passes through the center of mass C, the line of action of the impact impulse S intersects the x-axis at point K with an included angle θ, and OC=b, OK=h.

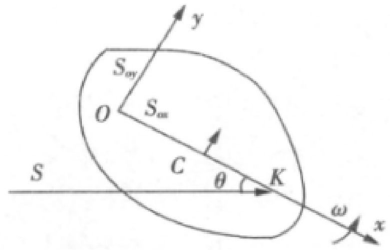

Figure 1. Simplified Fixed-axis Rotating Rigid Body for Projectile Wing In-position Deployment Impact

Based on the theorem of angular impulse and momentum

$$I_z\Omega - I_z w = Sh\sin\theta \tag{4}$$

the change in angular velocity is expressed as

$$\Omega - w = Sh\sin\theta / I_z \tag{5}$$

Then, the constraint impulses Sox and Soy are derived by applying the impulse-momentum theorem

$$0 = S_{ox} + S\cos\theta$$

$$mb(\Omega - w) = S_{oy} + S\sin\theta \tag{6}$$

from which we obtain the solutions:

$$S_{ox} = -S\cos\theta, S_{oy} = \left(\frac{mbh}{I_z} - 1\right)S\sin\theta \tag{7}$$

Obviously, to avoid generating an impact impulse at the bearing O (i.e., Sox = Soy = 0), it is essential that θ = π/2. In other words, the external impact impulse S must be perpendicular to the x-axis (i.e., the line OC), and the following condition must be satisfied:

$$h = I_z / mb \tag{8}$$

It can be concluded that the external impact impulse S acting on the rigid body must be perpendicular to the line connecting the rotation axis O and the center of mass C, and the distance h between the line of action of S and the axis O should comply with Equation (8). In this case, the intersection point K of S and the line OC is referred to as the center of percussion.

Assuming that the mass of the projectile wing is 2 kg, the moment of inertia Iz is 0.175 kg /m2, and the distance from the center of mass C of the projectile wing to the rotation axis center O is 0.5 m, it can be obtained that the center of percussion K is located on the line OC, with a distance h of 0.346 m from the rotation axis center.

3. Numerical Simulation Analysis of In-position Impact of Folding Wings

(1) Virtual Prototype Modeling of Folding Wings

To further analyze the in-position impact characteristics of folding wings, numerical simulations were carried out based on the Ansys multi-body dynamics virtual prototype simulation platform. The following assumptions were adopted in the establishment of the simulation model.

1) Since the projectile wing is made of composite materials and the buffer pad is made of rubber, the elastic modulus of

composite materials (on the order of GPa) is much higher than that of rubber (on the order of MPa). Therefore, compared with the impact deformation of the buffer pad, the impact deformation of the projectile wing is negligible. It is thus assumed that the projectile wing is a rigid body, the buffer pad is a deformable body, and the impact deformation is mainly caused by the buffer pad.

2) Given the symmetry of the left and right projectile wings and the assumption of synchronous deployment, only the single-wing loading condition was considered. Under the single-wing loading condition, the number of tie rods was reduced from two to one, which means the constraint force of the corresponding tie rod was halved. In addition, the guide sleeve-spring assembly is shared by the left and right projectile wings, so its mass was halved for symmetric analysis.

3) Due to the effect of the locking device, the impact deformation between the projectile wing and the buffer pad was small. In the direction of impact deformation, the deformable depth of the collision was 8 mm, and the small elastic deformation assumption was applied in the impact analysis.

During modeling, CATIA was used to establish the geometric models of each component of the projectile wing deployment and impact mechanism. Then, kinematic constraints were applied to the models, and the main kinematic pairs considered are as follows.

1) Fixed constraints: Including the constraint between the buffer pad and the mounting plate, and the constraint between the spring and the guide sleeve.

2) Revolute constraints: The constraint between the center of the projectile wing rotating shaft and the guide sleeve, the constraint between one end of the tie rod and the rotating shaft, and the constraint between the other end of the tie rod and the guide sleeve.

3) Translational constraints: The constraint between the guide shaft and the spring.

(2) Collision Simulation of the Guide Sleeve and Buffer Pad

The collision effect between the guide sleeve and the buffer pad is simulated using a collision force function. The restitution force function of the two colliding objects is defined as:

$$F = \begin{cases} 0, \quad q > q_0 \\ k(q_0 - q)^e - c_{\max} \cdot \left(\dfrac{dq}{qt} \right) \cdot \\ step(q, q_0 - d, 1, q_0, 0), \quad q \le q_0 \end{cases} \tag{9}$$

In the above formula: k is the stiffness coefficient, which characterizes the elastic force exerted per unit of deformation;

e is the elastic force deformation exponent, which represents the exponential growth law of the elastic force component with deformation and is generally assigned a value greater than 1;

Cmax is the damping coefficient, a parameter characterizing the damping force, which refers to the damping force exerted per unit of velocity;

d is the deformation distance triggering damping action, usually taking a very small value.

Therefore, the key to accurately simulating the collision effect lies in the selection of collision function parameters. In particular, after selecting other parameters according to the recommended values, the main task is to determine the appropriate stiffness coefficient k.

The impact between the guide sleeve and the buffer pad can be approximately regarded as a flat plate extruding a cylinder fixed at one end, as shown in Figure 2.

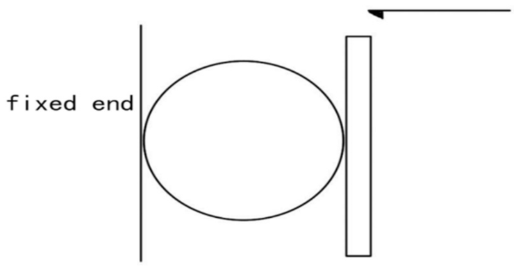

Figure 2. Simplified Fixed-axis Rotating Rigid Body for Projectile Wing In-position Deployment Impact

Based on the contact deformation in classical elasticity theory, the relationship between the deformation and contact force when a cylinder is compressed by two rigid flat plates is expressed as:

$$\frac{\delta}{R} = \gamma^2 \left[\ln\left(\frac{4}{\gamma} \right) - \frac{1}{2} \right] + \frac{9\gamma^4}{32} \tag{10}$$

$$\gamma = \left(\frac{2vP}{\pi R} \right)^{1/2} \tag{11}$$

$$v = \frac{2(1-\mu^2)}{E} \tag{12}$$

In the above formula: δ is the deformation distance of the buffer pad;

R is the radius of the buffer pad; L is the length of the buffer pad;

E and μ are the elastic modulus and Poisson's ratio of the buffer pad, respectively;

P is the impact force per unit length.

Since the impact duration is relatively short, the effects of aerodynamic force and friction force are neglected during the impact process.

Assuming that the rotational velocity of the projectile wing at impact is ω, it can be derived from the aforementioned angular momentum equation that:

$$\frac{d(Iw)}{dt} = -PL_{arm}$$

Based on $w = \dfrac{V}{L_{dist}}$, it can be concluded that

$$\frac{dv}{dt} = -\frac{PL_{arm}L_{dist}}{I} \tag{13}$$

In the above formula: Larm is the moment arm of the impact force relative to the rotation center;

Ldist is the distance from the impact point to the rotation center;

I is the moment of inertia of the projectile wing about the rotation center.

As such $\dfrac{d\delta}{dt} = v$, it follows that

$$\frac{d^2\delta}{dt^2} - \frac{PL_{arm}L_{dist}}{I} \tag{14}$$

By combining Equations (10) to (14) and specifying the actual calculation conditions, the curve of collision force varying with deformation depth during the entire collision process can be obtained, as shown in Figure 3.

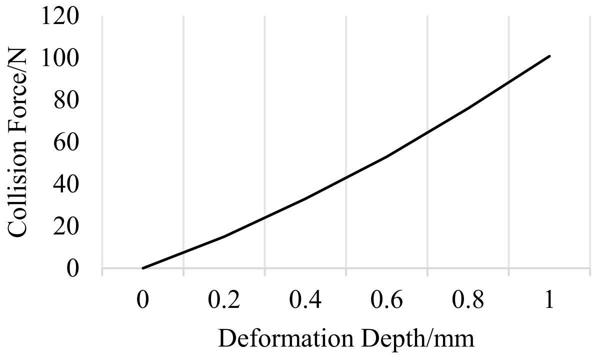

Figure 3. Curve of Collision Force versus Deformation Depth

It can be seen from the curve in Figure 3 that: with the ideal small deformation model adopted, the curve of collision force varying with deformation depth is basically linear. That is to say, under the premise of small deformation less than 10 mm, the stiffness coefficient can be regarded as a constant value. By performing linear fitting on this curve, the required stiffness coefficient k=100N/mm can be obtained, and then other collision force function parameters can be derived according to the recommended settings.

(3) Simulation Analysis of In-position Impact of Folding Wing Deployment

After establishing the collision model of the guide sleeve and buffer pad, the collision simulation analysis of the folding wing deployment mechanism can be carried out. First, the initial motion conditions of the collision process are given based on the analysis results of the projectile wing deployment dynamics, and then the dynamic simulation of the collision process is performed to study the collision characteristics under ideal working conditions. It is assumed that the timing starts at the moment when the guide sleeve comes into contact with the buffer pad; the collision duration is about 0.1s, and a step size of 0.001s is adopted for the simulation analysis.

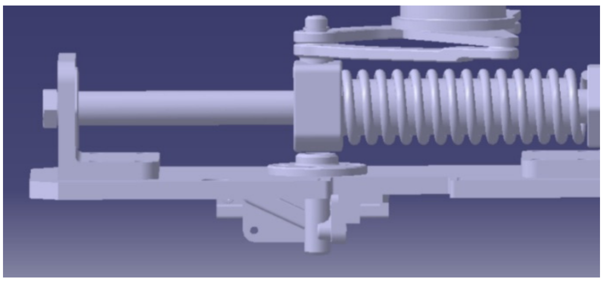

Figure 4. Dynamic Analysis Model of the Folding Wing Deployment Mechanism

4. Results Analysis and Discussion

The results of the in-position impact analysis characteristics of the folding wing deployment mechanism are as follows.

It can be concluded from the above figures that after the projectile wing deploys to the specified angle, the guide sleeve collides with the buffer pad, and the stress on both the guide sleeve and the baffle of the mounting plate decreases significantly. The maximum collision force occurs when the deformation depth reaches 7.64 mm, with a collision duration of 0.1 s and a magnitude of 770 N, which is basically consistent with the theoretical calculation results. Since the upper limit specified in the design is 5000 N, the design requirements are well satisfied.

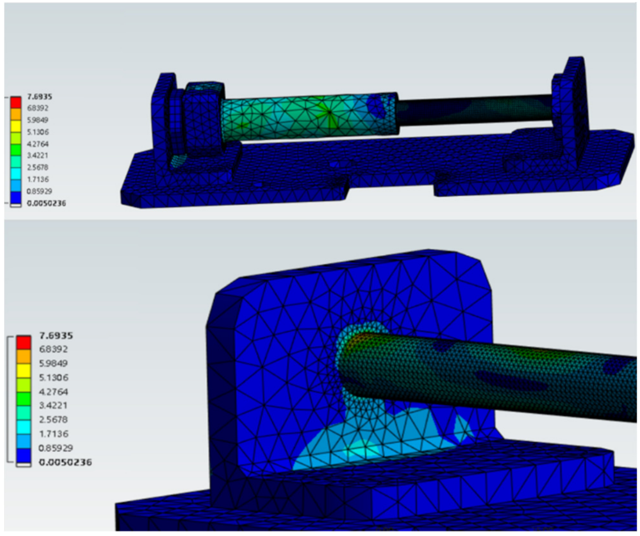

Figure 5. Stress Cloud Diagram of Dynamic Analysis for the Folding Wing Deployment Mechanism

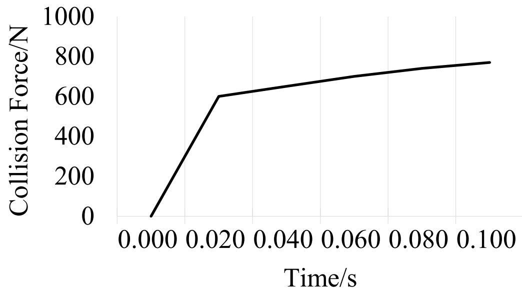

Figure 6. Curve of Absolute Value of Collision Force versus Time

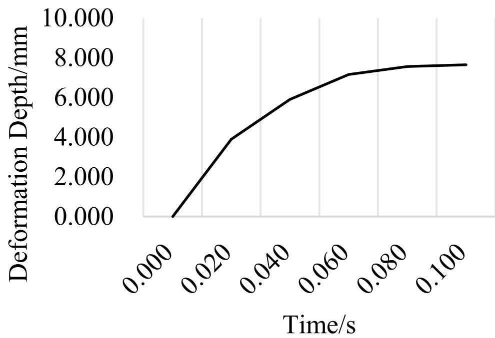

Figure 7. Curve of Buffer Pad Deformation Depth versus Time

During the entire process, the collision force rises smoothly without severe fluctuations, indicating that the buffer pad is rationally designed and can effectively absorb impact energy, thus reducing the risk of structural damage. However, when the buffer pad is compressed to its maximum limit, it will rebound against the guide sleeve, which is prone to causing angular velocity oscillation of the wing. The buffer pad alone can only reduce the impact force at the moment of in-position deployment. To position the wing at the designed deployment angle, an additional impulse is required, which will be borne by the locking pin mechanism. Therefore, for the design of the locking pin, it is imperative to verify its impact shear strength.

If different deployment times are required for different deployment environments and conditions, springs with different performance specifications will be needed. Using the same calculation method as described above, a simulation analysis was conducted on the in-position impact characteristics of four types of springs with distinct stiffness coefficients. The main calculation results of the impact characteristics are presented in the table below.

By comparing and analyzing the simulation results of springs with different performances, it can be concluded that: on the premise that the mechanical properties of other components remain unchanged, the higher the spring stiffness coefficient is, the greater the impact velocity of the guide sleeve and the deployment angular velocity of the wing will be; the larger the peak collision force will be at the same deformation depth, and the shorter the overall collision duration will be. Therefore, changing the spring performance can significantly alter the peak collision force load.

Table 1. Results of Impact Characteristics of Four Types of Springs with Different Stiffness Coefficients

spring stiffness coefficient/ N/mm	peak collision force/N	maximum deformation depth/mm	The Time Corresponding to the Maximum Deformation Depth/s
6	626	7.52	0.109
7	709	7.60	0.107
8	770	7.64	0.100
9	893	7.69	0.096

5. Conclusion

For ideal working conditions, the dynamic characteristics of the guide sleeve and buffer pad within an 8 mm collision stroke when the folding wing deployment mechanism reaches the in-position state were analyzed. The collision duration was determined to be 0.1 s, and the peak collision force was 770 N, which is lower than the design upper limit of 5000 N, thus satisfying the safety requirements for the peak collision force.

The spring stiffness coefficient is the key factor affecting the peak collision force. On the premise of meeting the deployment time requirements, reducing the impulse of the projectile wing before collision is the fundamental approach to solve the problem of collision overload of the projectile wing. Within a very short collision stroke, the buffer pad only functions to damp vibrations and reduce impact. It is therefore imperative to adopt a locking mechanism to lock the wing after it is fully deployed, and the impact effect should be taken into account in the strength design of the locking pin.

Considering that certain simplifications and assumptions were made for the collision model and material properties in the simulation calculations, these simplifications and assumptions are bound to exert a certain influence on the results of the collision analysis and introduce a certain degree of error. However, as qualitative conclusions, the findings presented herein have certain reference value for the analysis of folding mechanisms.

Acknowledgments

The authors sincerely thank Professor Qin Yanbin for his valuable guidance in the writing of this paper, and express gratitude to He Jialin for being a beam of light in the darkness during the process.

References

[1] Yang B Y. Measuring the Deployment Time of Folding Wings Using an Accelerometer[J]. Aerospace Shanghai,1993, (05): 25-26. DOI:10.19328/j.cnki.1006-1630.1993.05.005.

[2] Lv T G, Zhang X W, Li Y W, et al. Research on Motion Characteristics of Longitudinal Double-Folding Wings[J]. Aero Weaponry, 2023, 30(05): 127-134. DOI:10. 12132/ ISSN. 1673-5048.2023.0074.

[3] Song H X, Jin L. Dynamic Modeling and Stability Control of Folding-Wing Aircraft[J]. Acta Mechanica Sinica, 2020, 52 (06): 1548-1559.

[4] Xie Y M, Cheng X F, Zhang H W. Development of an Automatic Tension Measuring Device for Folding Wings[J]. Aerospace Technology, 2001, (02): 39-42.

[5] Zhen W Q, Ji Y Q, Shi Y G. Dynamic Simulation and Experimental Research on Deployment Process of Missile Folding Wings[J]. Acta Armamentarii, 2016, 37(08): 1409-1414.

[6] Guo X L, Pei J H, Yang Z Q, et al. Research on Deployment Kinematic Characteristics of UAV Folding Wings[J]. Journal of Nanjing University of Aeronautics and Astronautics , 2006, (04): 438-441.DOI:10.16356/j.1005-2615.2006. 04.009.

[7] Deng H L, Hu M, Chen W H, et al. Dynamic Simulation and Experimental Analysis of Folding Wing Deployment Mechanism Based on SimMechanics[J]. China Sciencepaper, 2015, 10(22): 2619-2623.

[8] Hangyue Z, Yanchu Y .Dynamic analysis of wing deployment of high altitude balloon launched small size folding-wing UAV1[J].MATEC Web of Conferences,2018, 19805004. DOI: 10.1051/matecconf/201819805004.

[9] Li L, Ren C X, Zhang D. Dynamic Simulation and Optimization of Folding Wing Mechanism Deployment[J]. Structure & Environment Engineering, 2007, (01): 17-21.

[10] Chen L Q. Analytical Mechanics Content in Theoretical Mechanics: Practice of Theoretical Mechanics Course [C]//Chinese Society of Theoretical and Applied Mechanics. Abstracts of the Chinese Mechanics Congress 2025 (Volume 1). Department of Mechanics, School of Mechanics and Engineering Science, Shanghai University, 2025: 31. DOI: 10. 26914/c.cnkihy.2025.058750.

[11] Chen L, Wang T, Sun Q X. Design and Analysis of a Spring Locking Mechanism for Folding Wings[C]//Jiangxi Society of Aeronautics, Structural and Strength Branch of Chinese Society of Aeronautics, Shaanxi Society of Aeronautics. Proceedings of the 2013 China Society of Aeronautics Structural Strength Academic Exchange Conference. Hongdu Aviation Industry Group, 2013: 7.

[12] Zhang Q, Nie H, Zhang M, et al. Dynamic Analysis of UAV Folding Wing Deployment[J]. Mechanical Design and Manufacturing Engineering, 2015, 44(02): 12-16.

[13] Nie W C, Cai W J, Zhang Y Q, et al. LS-DYNA-based Dynamic Analysis Method for Folding Wings[J]. Journal of Underwater Unmanned Systems, 2018, 26(04): 298-303.